CMOS, the thicknesses of the upper and lower buried-oxide layers, formed by $^{16}O^+$ implantation, were 0·47 and 0·43 μm, respectively. The active Si and Si shield layers were epitaxially grown, controlling the thicknesses to 0·4 and 0·23 μm, respectively. The gate oxide thickness was 50 nm. The gate lengths of the high-voltage CMOS and low-voltage CMOS were 5 and 2 μm, respectively. The offset-gate length L_{OFF} was 5 or 12 μm. The channel impurity concentrations for the *n*MOSFET and the *p*MOSFET were $5{\cdot}3 \times 10^{16}$ and $3{\cdot}7 \times 10^{16}$ cm^{-3}, respectively. Turning to the UMOS, the gate oxide thickness was 100 nm. The depths of the n^+-source and *p*-body regions were 1 and 3 μm, respectively. The width of the rectangular trench was 1·5 μm and its repeat spacing was 7·5 μm.

Electrical characteristics: Fig. 2 shows the substrate voltage V_{SUB} dependence of the threshold voltage V_{TH} for the low-voltage CMOS. When the voltage of the Si shield layer V_{SHI} is equal to the source voltage V_S, V_{TH} is independent of V_{SUB} varying from −100 to 100 V. However, when $V_{SHI} = V_{SUB}$, V_{TH} is greatly affected by V_{SUB} because V_{SUB} is applied to the upper buried-oxide layer. In this case, the *n*MOSFET changes from normally-off operation to normally-on with V_{SUB} in excess of approximately 18 V. For the *p*MOSFET, the same change occurs with a V_{SUB} of less than approximately −20 V.

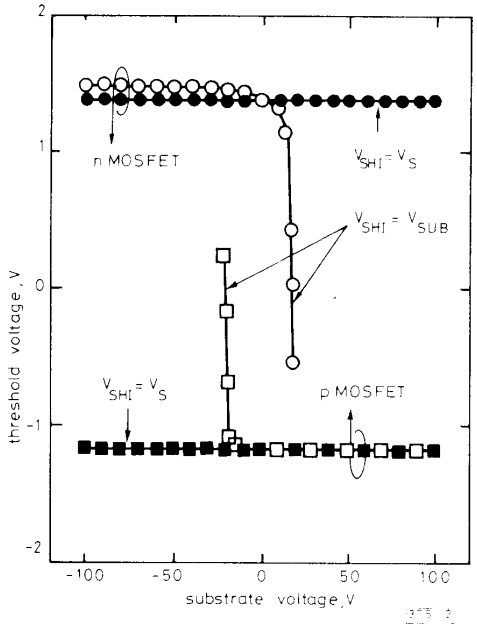

Fig. 2 *Dependence of threshold voltages on substrate voltages for low-voltage CMOS/SIMOX*

$V_S = 0$ V, $V_D = \pm 0{\cdot}1$ V

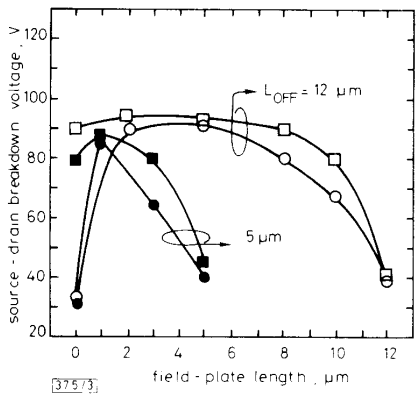

Fig. 3 *Dependence of breakdown voltages on field-plate lengths for high-voltage CMOS/SIMOX*

○● nMOSFET □■ pMOSFET

These results indicate that the CMOS can be implemented with the UMOS on one chip when $V_{SHI} = V_S$.

Fig. 3 shows the source-drain breakdown voltage BV_{DSS} for the high-voltage CMOS as a function of the length of the field plate connected to the gate. These characteristics showed almost no change even though V_{SUB} was varied from −100 to 100 V. A BV_{DSS} of more than 80 V is obtained by optimising L_{OFF} and the field-plate length.

Fig. 4 shows the gate voltage V_G dependence of the specific on-resistance as a parameter of V_{TH} for the UMOS with $BV_{DSS} = 82$ V. The specific on-resistance is affected by V_G and V_{TH}, but is realised with 2–3·5 mΩ cm^2 at a V_G of more than 15 V.

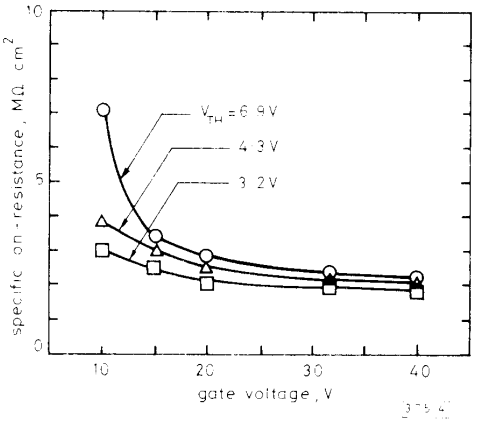

Fig. 4 *Dependence of specific on-resistance on gate voltage for UMOS*

Conclusion: A new SIMOX isolation structure aimed at the realisation of a completely latch-up-free IPLSI has been demonstrated. The electrical characteristics of the CMOS/SIMOX were not degraded even varying the substrate voltage from −100 to 100 V. Furthermore, the breakdown voltages of the high-voltage CMOS/SIMOX and the vertical power UMOS/bulk were more than 80 V. From these results, it is anticipated that an 80 V SIMOX IPLSI fabricated with a one-chip process will soon be realised.

Acknowledgment: We would like to thank T. Sakai for discussions and encouragement.

T. OHNO
S. MATSUMOTO
K. IZUMI

NTT LSI Laboratories
3-1 Morinosato Wakamiya, Atsugi-shi, Kanagawa 243-01, Japan

30th June 1989

References

1 OHATA, Y., and IZUMITA, T.: 'Dielectrically isolated intelligent power switch'. Proceedings of the custom integrated circuit conference, Portland, 1987, pp. 443–446

2 IZUMI, K., DOKEN, M., and ARIYOSHI, H.: 'CMOS devices fabricated on buried SiO_2 layers formed by oxygen implantation into silicon', *Electron. Lett.*, 1978, **14**, pp. 593–594

3 CHANG, H. R., BLACK, R. D., TEMPLE, V. A. K., TANTRAPORN, W., and BALIGA, B. J.: 'Self-aligned UMOSFET's with a specific on-resistance of 1 mΩ . cm^2', *IEEE Trans. Electron Devices*, 1987, **ED-34**, pp. 2329–2333

GENERALISED 1/*f* SHOT NOISE

Indexing terms: Semiconductor devices and materials, Noise

We define a generalised form of 1/*f* shot noise, which can serve as a source of $1/f^{\alpha}$ noise for α in the range $0 < \alpha < 2$, and present its first-order amplitude probability density function. For some parameters of the power-law-decaying impulse-response function, the amplitude has a Lévy-stable probability density function.

Introduction: $1/f$ noise is present in many semiconductor devices under a variety of experimental conditions. One widely used theoretical approach to this problem makes use of a superposition of relaxation processes of different time-constants.[1-3] An alternative approach, suggested by Schönfeld[4] and considered further by van der Zeil,[5] entails the use of shot noise with an impulse-response function that decays as $t^{-1/2}$.

In this letter, we obtain explicit results for the power spectral density associated with generalised $1/f$ shot noise, in which the impulse-response function decays as $t^{-\beta}$, with $0 < \beta < 1$. Generalised $1/f$ shot noise exhibits a power spectral density that varies as $1/f^{\alpha}$ $(0 < \alpha < 2)$ with $\alpha = 2(1-\beta)$. Finally, we consider the amplitude probability density function for $1/f$ shot noise.

Definition: $1/f$ shot noise $I(t)$ may be expressed as an infinite sum of power-law impulse response functions

$$I(t) \equiv \sum_{j=-\infty}^{\infty} h(t - t_j) \tag{1}$$

where

$$h(t) \equiv \begin{cases} Kt^{-\beta} & 0 < t < B \\ 0 & \text{otherwise} \end{cases} \tag{2}$$

and the times t_j are random events from a homogeneous Poisson point process of rate μ. The parameters B, K and β are deterministic and fixed. We focus on the range of β between 0 and 1; the behaviour of this shot noise for $\beta > 1$ is fundamentally different and will be considered elsewhere.[6] For all calculations we assume that t is finite, so that the shot-noise process has reached a steady state.

Power spectral density: The power spectral density $S_I(f)$ of the shot-noise process $I(t)$, obtained from Carson's theorem,[7] is given by

$$\begin{aligned} S_I(f) &= \langle I \rangle^2 \delta(f) + \mu \left| \int_{-\infty}^{\infty} h(t) e^{-j2\pi ft}\, dt \right|^2 \\ &= \langle I \rangle^2 \delta(f) + \mu K^2 \\ &\quad \times |\Gamma(\alpha/2) - \Gamma(\alpha/2, j2\pi fB)|^2 (2\pi f)^{-\alpha} \end{aligned} \tag{3}$$

where $\delta(.)$ is the Dirac delta function, $\Gamma(.,.)$ is the incomplete gamma function defined by

$$\Gamma(a, x) \equiv \int_x^{\infty} e^{-t} t^{a-1}\, dt \tag{4}$$

and the angular brackets $\langle . \rangle$ represent ensenble averaging with respect to I. In the limit $f \to 0$, by definition the power spectral density approaches a constant value

$$S_I(f) \to \mu \left[\int_{-\infty}^{\infty} h(t)\, dt \right]^2 = \mu K^2 \frac{B^{-\alpha}}{(\alpha/2)^2} \qquad f \to 0 \tag{5}$$

In the limit $f \to \infty$, the incomplete gamma function in eqn. 3 approaches zero, so that

$$S_I(f) \to \mu K^2 \Gamma^2(\alpha/2)(2\pi f)^{-\alpha} \qquad f \to \infty \tag{6}$$

Thus, for high frequencies f the power spectral density does indeed behave as $1/f^{\alpha}$, with α defined as above.

If we set the cutoff of the impulse-response function B to ∞, we obtain the same $1/f^{\alpha}$ behaviour for all frequencies, the power spectral density being

$$S_I(f) = \langle I \rangle^2 \delta(f) + \mu \langle K^2 \rangle \Gamma^2(\alpha/2)(2\pi f)^{-\alpha} \tag{7}$$

This form of the impulse-response function was previously considered only for the special case $\alpha = 1$, by Schönfeld.[4]

In this limit, however, the power spectral density has infinite energy. This poses a problem that can be solved in one of three ways. First, the impulse-response function may be truncated at a finite value B, as we have suggested by the definition in eqn. 2. Second, the area of the impulse-response function may be made finite by multiplying it by an exponentially decaying function

$$h^*(t) \equiv Kt^{-\beta} e^{-\omega_0 t} \tag{8}$$

as considered by Buckingham,[7] which yields

$$S_I^*(f) = \langle I \rangle^2 \delta(f) + \mu K^2 \Gamma^2(\alpha/2)[\omega_0^2 + (2\pi f)^2]^{-\alpha/2} \tag{9}$$

Again the power spectral density is bounded in the neighbourhood of $f = 0$ and behaves as $1/f^{\alpha}$ for high frequencies. Finally, the physical limitations of any real experiment used to measure the power spectral density may be imposed on the system. Since the experiment must be conducted in finite time, those components of the power spectral density with frequencies lower than the reciprocal of the duration of the experiment will be excluded. Similarly, since any measuring apparatus has a finite frequency response, those components of the power spectral density at high frequencies will also be excluded. Since the power spectral density is effectively truncated at both low and high frequency limits, the total energy will be finite for any value of α: $0 < \alpha < 2$ and any possible experimental measurement.[5]

Fig. 1 shows the shot-noise power spectral densities obtained with $\alpha = 1$ for three types of $1/f$ impulse-response functions: no cutoff (eqn. 2, $B = \infty$), abrupt cutoff (eqn. 2, $B < \infty$) and exponentially decaying power law (eqn. 8). The power spectral densities all take the form of $1/f^{\alpha}$ with exponent $\alpha = 1$ for high frequencies. Note that the abrupt cutoff in the time domain gives rise to ringing in the frequency domain.

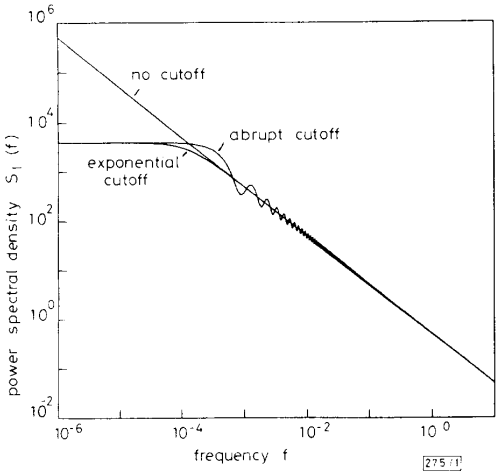

Fig. 1 *Power spectral densities for 1/f shot noise with different cutoffs: A = 0 and B = ∞, A = 0 and B = 1000, and exponential cutoff with* $\omega_0 = \pi/4000$

Note that power spectral densities are power-law with exponent α for high frequencies, and that abrupt cutoff in impulse-response function gives rise to ringing in frequency domain

Amplitude probability density function: We now consider the first-order amplitude statistics of the shot-noise process I. The first-order moment generating function $Q_I(s)$, calculated from the definition,[9] is given by[6]

$$\begin{aligned} Q_I(s) &\equiv \langle e^{-sI} \rangle \\ &= \exp\left[-\mu B + \mu (sK)^{1/\beta} \Gamma(-1/\beta, sKB^{-\beta})/\beta \right] \end{aligned} \tag{10}$$

First-order amplitude statistics may be numerically computed from this moment generating function.

When $B \to \infty$, the shot-noise process I not only has infinite energy, as stated above, but is also infinite with probability one. In that case, the moment generating function $Q_I(s)$ in eqn.

10 becomes

$$Q_I(s) \equiv \begin{cases} 1 & s = 0 \\ 0 & s \neq 0 \end{cases} \tag{11}$$

whereon

$$\Pr\{I < x\} = 0 \qquad \text{for all } x < \infty \tag{12}$$

However, for other infinite-area impulse-response functions the resulting shot noise does not have trivial amplitude properties.[6] For $B = \infty$ and $\beta > 1$ the resulting shot noise has a (finite) Lévy-stable amplitude probability density (and therefore does not converge to Gaussian form, even in the limit $\mu \to \infty$). In that case we integrate the incomplete gamma function in eqn. 10 by parts and use l'Hôpital's rule to obtain

$$Q_I(s) = \exp\left[-\mu(sK)^{1/\beta}\Gamma(1 - 1/\beta)\right] \tag{13}$$

This moment generating function is of the form

$$Q(s) = \exp\left[-cs^D\right] \tag{14}$$

where c is a constant, and therefore for all μ the shot noise I is a Lévy-stable random variable with extreme asymmetry[6] of dimension $1/\beta$: $0 < 1/\beta < 1$. Thus an infinite-area impulse-response function may be used to construct a shot-noise process which has nontrivial and non-Gaussian amplitude properties for all driving rates μ.

The difference between trivial and nontrivial amplitude properties appears to lie in the nature of the infinity in the impulse-response function. For $\beta < 1$, the infinite area is in the tail, which lasts for infinite time. Since the tails of previous impulse-response functions are always present, the process is always infinite. However, for $\beta > 1$, the infinite area is contained in the infinitesimal neighbourhood of $t = 0$, and therefore only manifests itself at the times $t = t_j$ corresponding to the events of the driving homogeneous Poisson point process. The remainder of the time the process is finite.

Conclusion: We have defined a generalised form of $1/f$ shot noise, for which the associated impulse-response functions assume a decaying power-law form with power $-\beta$. For $0 < \beta < 1$, the $1/f$ shot-noise process can serve as a source of $1/f^{\alpha}$ noise, for any $\alpha \equiv 2(1 - \beta)$ in the range $0 < \alpha < 2$. The first-order moment generating function is given for $0 < \beta < 1$, from which first-order statistics may be numerically computed. Finally, for $\beta > 1$ and $B \to \infty$ we show that the amplitude has a Lévy-stable probability density function.

Acknowledgments: This work was supported by the National Science Foundation through the Center for Telecommunications Research and by the Joint Services Electronics Program through the Columbia Radiation Laboratory.

S. B. LOWEN
M. C. TEICH
Department of Electrical Engineering
Columbia University
500 West 120th Street, New York, NY 10027, USA

15th June 1989

References

1 VAN DER ZEIL, A.: 'On the noise spectra of semi-conductor noise and of flicker effect', *Physica*, 1950, **16**, pp. 359–372
2 MCWHORTER, A. L.: '$1/f$ noise and related surface effects in germanium', *in* KINGSTON, R. H. (Ed.): 'Semiconductor surface physics' (Univ. of Penn. Press, Philadelphia, 1956)
3 WEISSMAN, M. B.: '$1/f$ noise and other slow, nonexponential kinetics in condensed matter', *Rev. Mod. Phys.*, 1988, **60**, pp. 537–571
4 SCHÖNFELD, H.: 'Beitrag zum $1/f$-Gesetz beim Rauschen von Halbleitern', *Z. Naturforsch.*, 1955, **A10**, pp. 291–300
5 VAN DER ZEIL, A.: 'Flicker noise in electronic devices', *Adv. Electron. & Electron Phys.*, 1979, **49**, pp. 225–297
6 LOWEN, S. B., and TEICH, M. C.: manuscript in preparation
7 RICE, S. O.: 'Mathematical analysis of random noise', *Bell Syst. Tech. J.*, 1944, **23**, pp. 1–51; 1945, **24**, pp. 52–162; reprinted in WAX, N. (Ed.): 'Selected papers on noise and stochastic processes' (Dover, New York, 1954), pp. 133–294
8 BUCKINGHAM, M. J.: 'Noise in electronic devices and systems' (Wiley-Halsted, New York, 1983)
9 SALEH, B. E. A., and TEICH, M. C.: 'Multiplied-Poisson noise in pulse, particle, and photon detection', *Proc. IEEE*, 1982, **70**, pp. 229–245
10 FELLER, W.: 'An introduction to probability theory and its applications' (Wiley, New York, 1971), Vol. 2, 3rd edn.

CMOS CIRCUIT DESIGN OF PROGRAMMABLE NEURAL NET CLASSIFIER OF 'EXCLUSIVE' CLASSES

Indexing terms: Neural networks, Artificial intelligence, Networks, Pattern recognition

A circuit implementation of a pattern classifier based on the Hamming net is proposed. The circuit classifies pattern configurations representing the digits 0, ..., 9; it is based on a standard CMOS technology and it allows a simple and reliable implementation. The circuit has been simulated by using SPICE; it exhibits notable robustness, since its functionality is not affected by parameter variations in a wide range.

Introduction: The possibility of implementing electronic neural networks has recently received considerable attention from the VLSI designers' community. Among the various solutions,[1–4] the possibility of implementing these systems through standard CMOS processes seems particularly appealing. A major requirement for any implementation lies in the possibility of adapting synaptic strengths to the specific problem considered. To this end electronically programmable synapses[5] should be used.

In this letter we study a neural network implementation (at the transistor level), of a programmable exclusive classifier (the meaning of 'exclusive' will be clarifed in the following). Being interested in scaling up the complexity of the neural network, this study considers a simple implementation of both neurons and synaptic links. The approach proved successful, as the architectural specifications for the classifier were only marginally affected by these choices.

Principles: A classifier determines which of M classes is most representative of a given input pattern. Using bit-maps of the pattern, the minimum error classifier[6] calculates the Hamming distance of the input pattern to the exemplary pattern of each class (i.e. the number of input bits which do not match the corresponding exemplary bits), and selects the class at the minimum Hamming distance. A two-layer neural net implementation of this classifier is shown in Fig. 1: it is called a Hamming net.[6] The input–output characteristics of neurons are of the threshold logic type and exhibit a finite gain. The jth node ($1 \leq j \leq M$) of the lower subnet calculates $(1 - HD_j/N)$, where HD_j is the Hamming distance of the input

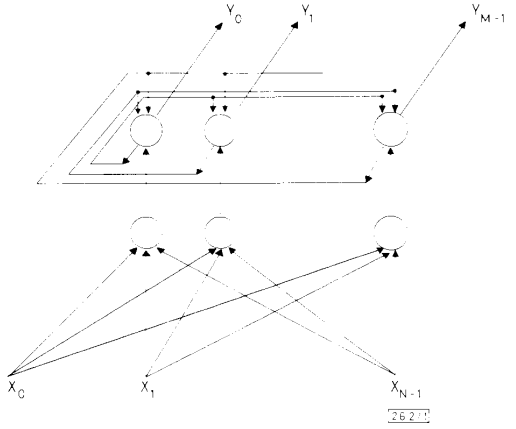

Fig. 1 *Hamming net classifier*